Vol. **112** (2007) *ACTA PHYSICA POLONICA A* No. 2

Proceedings of the XXXVI International School of Semiconducting Compounds, Jaszowiec 2007

Optically Pumped Laser Action on Nitride Based Separate Confinement Heterostructures Grown along the $(11\bar{2}0)$ Crystallographic Direction

H. Teisseyre[a], M. Szymański[b], A. Khachapuridze[a], C. Skierbiszewski[a], A. Feduniewicz-Żmuda[a], M. Siekacz[a], B. Łucznik[a], G. Kamler[a], M. Kryśko[a], T. Suski[a], P. Perlin[a], I. Grzegory[a] and S. Porowski[a]

[a]Institute of High Pressure Physics
Sokołowska 29/37, 01-142 Warsaw, Poland
[b]Institute of Electron Technology
al. Lotników 32/46, 02-668 Warsaw, Poland

The intention of this work is to discuss and report on our research on nonpolar laser structures grown on bulk GaN crystal substrates along the $(11\bar{2}0)$ nonpolar direction. The main advantages of such nonpolar structures are related to the elimination of the built-in electric fields present in commonly used systems grown along the polar (0001) axis of nitride crystals. We demonstrated the optically pumped laser action on separate confinement heterostructures. Laser action is clearly shown by spontaneous emission saturation, abrupt line narrowing, and strong transversal electric polarization of output light. The lasing threshold was reached at an excitation power density of 260 kW/cm^2 for a 700 μm long cavity (at room temperature).

PACS numbers: 42.55.Px, 78.45.+h, 78.66.Fd

1. Introduction

Recent progress in growing nitrides along the nonpolar crystallographic direction has opened the way for a new generation of nitride optoelectronic devices free from built-in electric fields due to spontaneous and piezoelectric polarizations [1, 2]. To be exact, both polarizations are still present in nitride nonpolar structures but they do not induce any charges on the interfaces due to the fact that the

polar axis lies within the growth plane of the film. In optoelectronic devices grown along the classical polar direction, the built-in electric field results in the spatial separation of electron and hole wave functions and a reduction of the overlap of both wave functions, which in turn leads to a decrease in radiative efficiency.

A second reason for interest in lasers grown along a nonpolar direction is related to the increasing interest in polariton lasers [3, 4]. In a polariton laser, lasing states do not require a population inversion, therefore pumping thresholds may be much lower and are no longer related to the volume of the laser. The growth of *a*-plane and *m*-plane GaN/AlGaN quantum well (QW) structures on different substrates has been previously demonstrated [2]. Recently, two groups have reported laser action in samples grown along the nonpolar direction [5, 6]. However, there remains a lack of information concerning the basic properties of nonpolar laser structures.

2. Experimental method

To avoid problems related to a lattice mismatch between the substrate and laser structure, we used GaN bulk crystals. The bulk substrates were prepared in the following way. In the beginning we used low dislocation bulk GaN crystals grown from gallium nitride solutions under a high nitride pressure [7]. Unfortunately, such crystals are too thin to perform epitaxial growth in any direction perpendicular to the *c* axis, in other words along the nonpolar direction. To increase the thickness of these crystals we used a hydride vapor phase epitaxial (HVPE) method to overgrow them to a thickness of a few millimeters. Finally the substrates, in the form of strips with a length and width of a few millimeters, were cut along the appropriate crystallographic directions. The laser structures (separate confinement heterostructure laser) were grown by means of plasma assisted molecular beam epitaxy (PAMBE). The active region of the laser structure consists of five GaN ≈ 50 Å QWs with $Al_{0.04}Ga_{0.96}N$ barriers and was embedded in a 0.1 μm thick $Al_{0.04}Ga_{0.96}N$ light-guiding layer. At the top and bottom of the structure 0.35 μm cladding layers of $Al_{0.12}Ga_{0.88}N$ were grown. We also grew a second laser sample, which contained a structure identical to the first sample, except for a higher aluminum concentration in the waveguide and barriers (6% rather than 4%) and thinner quantum wells (2 nm rather than 5 nm).

The crystal quality of the samples was characterized by X-ray diffraction. The 2θ–ω scans were measured for $(11\bar{2}0)$ reflections. The main peak related to the GaN substrate and QW region was located at 57.77°, with two other peaks related to waveguide and cladding layers observed at a higher angle. The good agreement between the experimental results and simulated values indicates proper growth conditions, which were also confirmed later by transition electron microscopy studies.

Optical pumping experiments were performed on cleaved laser strips by using the fourth harmonic of an Nd:YAG laser (266 nm excitation). The pulse lengths

were 10 ns with a 20 Hz repetition rate. The pulse energy was controlled by an Ophir power meter. The laser beam was focused on the sample surface using a cylindrical lens, and the width of the laser strip was measured to establish the value of power density. Finally, the light emitted from the laser facet along the $(1\bar{1}00)$ crystallographic direction was analyzed by a CCD detector connected to a SPEX 500 spectrometer.

3. Results and discussion

The results of our optical pumping experiments at room temperature are shown in Fig. 1. The related stimulated emission spectra for both laser structures are recorded just above the lasing threshold, and we also show the spontaneous emission spectra for both lasers. The laser action mechanism is confirmed by the following experimental facts. First, for excitation power just above the lasing threshold we observed a multimode structure of the laser emission. Second, the laser line was fully transversal electric (TE) polarized. Third, we observed a narrowing of the spontaneous emission spectrum and a clear threshold for stimulated emission by optical pumping. Finally, for the first laser structure we observed changes of the energetic position of the stimulated emission with cavity length [8]. This is due to the fact that for different cavity lengths transparency conditions may be obtained for different values of the gain.

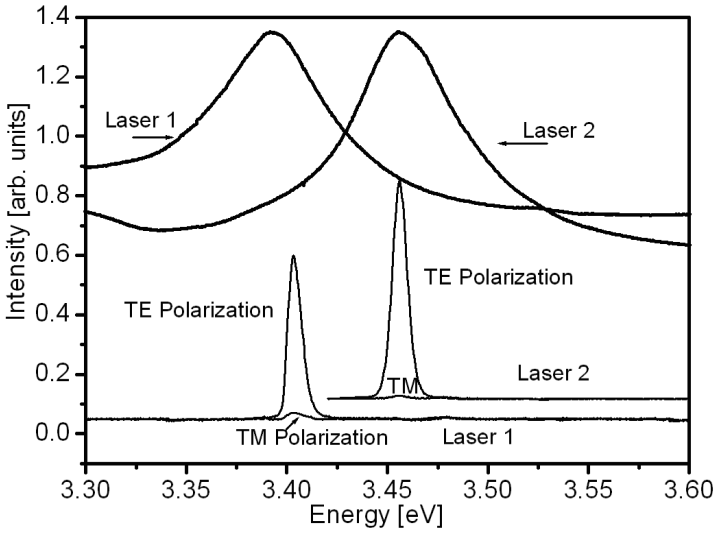

Fig. 1. Spectra of the stimulated emissions at room temperature for TE and transversal magnetic (TM) polarizations, for both types of laser described in the text obtained with the fourth harmonic of a Nd:YAG impulse laser. The two upper spectra represent the spontaneous emissions from both lasers obtained below the threshold for identical excitation.

The room-temperature laser emission spectra are located at 3.403 eV and 3.456 eV for laser 1 and laser 2, respectively. The energetic distance between both lines (53 meV) corresponds closely to the calculation results while using a simple flat band model (48 meV). This fact and changes of the energetic position of the laser emission peak for both lasers confirm that laser emission occurred at the active region of the laser structure, not in the bulk material of the substrate.

In Fig. 2 we represent the results of the optical pumping experiments, i.e. total intensity of the light output taken from a cleaved facet as a function of excitation laser power. For all our samples a clear sublinear growth of emission intensity was observed. From the first laser structure we cleaved strips of different cavity lengths (700, 500, 300 μm) in such a way that the cleavage mirrors were perpendicular to the $(1\bar{1}00)$ direction. The threshold pump power density was determined to be equal, respectively, to 260, 280, and 370 kW/cm^2 for the 700, 500, and 300 μm cavity length, respectively. For laser 2 the threshold pump power density was higher than for laser 1 and possessed a value of 500 kW/cm^2 for a 500 μm cavity strip.

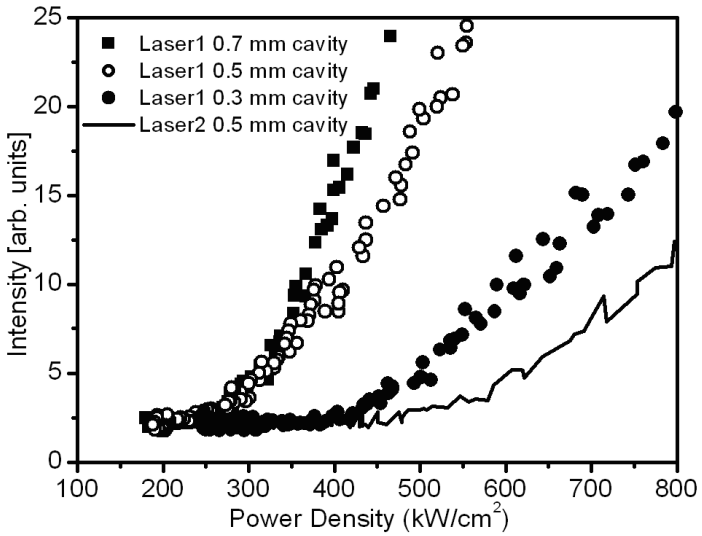

Fig. 2. Excitation power density dependence at room temperature for laser 1 and laser 2. Laser 1 was cleaved with 300, 500, and 700 μm laser cavities. Laser 2 possessed a 500 μm laser cavity.

There are a number of factors which affect the threshold in optical pumped laser structures. The higher threshold of laser 2 can be explained by a smaller confinement factor defined as the overlap of the optical mode with the active region [9]. In addition, the smaller contrast of the refractive indices between the waveguide (6% instead of 4% of aluminum) and cladding layer (12%) increases the threshold. As a result, the heterostructure of laser 2 supports a spatially

wider optical mode, undergoing gain in a smaller region, and a higher pumping power must be used to obtain lasing. This effect could be compensated (or rather minimized) by other effects described in the literature [10]. The refractive index for GaN–AlGaN alloys is strongly dependent on the wavelength of the laser emission. This effect is rather pronounced at wavelengths close to the GaN band gap. This leads to an increase in the refractive index contrast for laser 2, resulting in a lowering of the threshold. The higher threshold for laser 2 in comparison with laser 1 is due to the competition between all these effects.

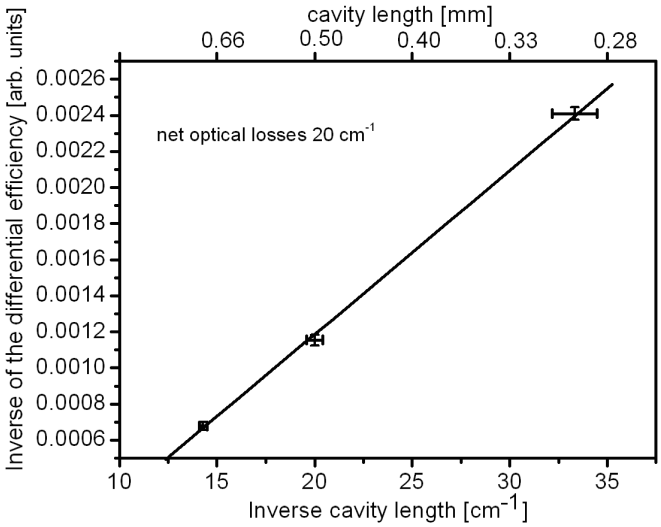

Fig. 3. Inverse of the differential efficiency as a function of the inverse cavity length for three different laser cavities (300, 500, and 700 μm cleaved from laser 1 sample). Solid line represents fitting with $\alpha = 20$ cm^{-1}.

In our experiments, by using different cavity lengths we were able to determine the optical losses in the first laser structure [11]. This may be achieved by measuring the differential efficiency as a function of the inverse cavity length (Fig. 3) and employing the following equation:

$$\eta_{\mathrm{m}}^{-1} = \frac{1}{kdC}\eta_{\mathrm{stim}}^{-1}\left(\frac{1}{L} + \frac{\alpha}{\ln(1/R)}\right),$$

in which η_{m} is the differential quantum efficiency, L — the cavity length, d is the width of the excitation strip, η_{stim} — internal quantum efficiency, R — the mirror reflectivity, and α — the net internal losses. The k coefficient is defined by the relation between power of the pumping light P_{in} and effective injection current density J by the relation $J = kP_{\mathrm{in}}$. We also should mention that in a real experiment we measure a quantity CP_{out} which is a composite of constant C and the real output power P_{out}. Finally, by using this method we were able to determine optical losses in the first laser structure to be at a level of 20 cm^{-1}.

4. Summary

In summary, GaN/AlGaN laser structures were grown by PAMBE along the $(11\bar{2}0)$ nonpolar crystallographic direction. On such structures we observed laser action and for one of them we established optical losses of 20 cm^{-1}. For the nonpolar laser we also measured a threshold power density in the range from 260 to 500 kW/cm^2. The value is still higher than the one reported in the literature for optically pumped polar structures [12], but more detailed studies are certainly required in order to compare both the polar and nonpolar systems.

Acknowledgments

This work was partially supported by project No. 1P03B 053 29 of the Polish Ministry of Science and Higher Education.

References

[1] P. Waltereit, O. Brandt, A. Trampert, H.T. Grahn, J. Menniger, M. Ramsteiner, M. Reiche, K.H. Ploog, *Nature* **406**, 865 (2000).

[2] G. Purvis, *III–V Review* **18**, 26 (2005) and references therein.

[3] S. Christopoulos, G. Baldassarri Hoger von Hogersthal, A.J.D. Grundy, P.G. Lagoudakis, A.V. Kavokin, J.J. Baumberg, G. Christmann, R. Butte, E. Feltin, J.-F. Carlin, N. Grandjean, *Phys. Rev. Lett.* **98**, 126405 (2007).

[4] G. Malpuech, A. Di Carlo, A. Kavokin, J.J. Baumberg, M. Zamfirescu, P. Lugli, *Appl. Phys. Lett.* **81**, 412 (2002).

[5] M.C. Schmidt, K.C. Kim, R.M. Farrell, D.F. Feezell, D.A. Cohen, M. Saito, K. Fujito, J.S. Speck, S.P. DenBaars, S. Nakamura, *Jpn. J. Appl. Phys.* **46**, L190 (2007).

[6] K. Okamoto, H. Ohta, S.F. Chichibu, J. Ichihara, H. Takasu, *Jpn. J. Appl. Phys.* **46**, L187 (2007).

[7] I. Grzegory, S. Krukowski, M. Leszczynski, P. Perlin, T. Suski, S. Porowski, in: *Nitride Semiconductors Handbook on Materials and Devices*, Eds. P. Ruterana, M. Albrecht, J. Neugabauer, Wiley, Weinheim 2003, p. 1.

[8] P. Alleysson, J. Cibert, G. Feuillet, Le Si Dand, *J. Cryst. Growth.* **159**, 672 (1996).

[9] B. Mroziewicz, M. Bugajski, W. Nakwaski, *Physics of Semiconductor Lasers*, North Holland, Amsterdam 1991, Ch. 4.1.5.

[10] G.M. Laws, E.C. Larkins, I. Harrison, *J. Appl. Phys.* **89**, 1108 (2001) and references therein.

[11] K. Kondo, M. Ukita, H. Yoshida, Y. Kishita, H. Okuyama, S. Ito, T. Ohata, K. Nakano, A. Ishibashi, *J. Appl. Phys.* **76**, 2621 (1994).

[12] S. Bidnyk, J.B. Lam, B.D. Little, Y.H. Kwon, J.J. Song, G.E. Bulman, H.S. Kong, T.J. Schmidt, *Appl. Phys. Lett.* **75**, 3905 (1999).